Asian Journal of Physical and Chemical Sciences

3(1): 1-16, 2017; Article no.AJOPACS.35542
ISSN: 2456-7779

Thermoluminescence Characteristics of Natural Quartz and Synthesized Silica Glass Prepared by Sol-Gel Technique

F. Khamis[1*] and D. E. Arafah[2,3]

[1]Department of Physics, University of Tripoli, Tripoli 13220, Libya.
[2]Al al-Bayt University, P.O.Box 130040, Mafraq 25113, Jordan.
[3]Department of Physics, The University of Jordan, Amman 11942, Jordan.

Authors' contributions

This work was carried out in collaboration between both authors. Both authors designed the study. Author FK preformed the statistical analysis, wrote the protocol and wrote the first draft of the manuscript. Both authors managed analysis of study and managed the literature searches. Both authors read and approved the final manuscript.

Article Information

DOI: 10.9734/AJOPACS/2017/35542
Editor(s):
(1) Mustafa Boyukata, Physics, Bozok University, Turkey.
Reviewers:
(1) Birsa Mihail Lucian, Alexandru Ioan Cuza University of Iasi, Romania.
(2) Subramaniam Jahanadan, Universiti Teknologi Malaysia, Malaysia.
(3) R. Masrour, Cady Ayyed University, Morocco.
(4) K. Rama Krishna, Malla Reddy College of Engineering & Technology, India.
Complete Peer review History: http://www.sciencedomain.org/review-history/20578

Original Research Article

Received 18th July 2017
Accepted 13th August 2017
Published 21st August 2017

ABSTRACT

Aims: Study of thermoluminescence (TL) characteristics of natural quartz and synthesized quartz (silica glass synthesized by sol-gel technique) was investigated.
Study Design: Studies TL properties of both types samples with different annealing temperatures, heating rates and doses actual samples experiment and an analysis of results.
Place and Duration of Study: Department of Physics (Atomic Physics Lab's, The University of Jordan), between May 2012 to May 2014.
Methodology: Natural and synthesized quartz annealed at high temperatures exhibit crystalline of natural as indicated by x-ray diffraction spectra and amorphous structure of synthesized silica glass and converted partially to crystalline form by irradiation. Examination was facilitated by use of EDS and SEM to validate the results and conclusions.

**Corresponding author: E-mail: khamesf@gmail.com, fawzeiak@yahoo.com;*

Results: TL-properties of quartz resulted in the formation of two TL-peaks centered near 150°C (P_1) and 200°C (P_2) whereas in synthesized glass, the detected peaks are centered near 150°C and about 300°C. Variations of the normalized TL intensity as function of the heating rate indicated reduction of TL-intensity accompanied by shift of TL-peaks towards higher temperatures. All glow (GL-) curve region was de-convoluted into five and six main peak components.
Conclusion: The results show agreement with the available literature data. The main emission TL-peaks of SiO_2 are largely associated with relaxation of excitons and oxygen defect sites related to shallow and deep trapping centers. The first peak, P_1, is due to band-to-band transition of electrons from the minimum of the conduction band to the valence band maximum (VBM). The second Peak, P_2, is attributed to relaxation of an exciton formed during ionization at a broken Si-O bond, and emission of self-trapped exciton occurs as a result of direct carrier re-combinations or via an oxygen vacancy. The other peaks, P_3-P_6, are associated with *E´*-centers that form sub-band states extending from shallow to deep levels in the band gap of SiO_2.

Keywords: Thermoluminescence; quartz; silica glass; sol-gel; trapping parameters.

1. INTRODUCTION

Thermoluminescence has been largely recognized to be useful, handy and efficient technique for obtaining information on the trapping and defect state distribution of insulating materials. In particular, Luminescence studies on quartz (crystalline and amorphous SiO_2 (a-SiO_2), have indicated the material to be an interesting host that exhibits pronounced influence on thermoluminescence (TL) response of dosimeters; and consequently, many of its exciting properties were characterized by: TL studies including dating and retrospective dosimetric applications [1-5], and their effects on thermal treatments [3,6] and kinetic analysis [5,7]. These experiments revealed that quartz exhibits a number of defect states and TL-peaks that varying number, intensity and positions. The results obtained from various forms of quartz types using several techniques indicate that there are variations in the shapes of the glow (GL-) curves obtained. Literature of different quartz types has, however, shown a cluster of peaks at temperatures ~ 60, 80, 100-110, 130, 180, 200-210, 230, 310 and 350°C, see Table 1. Although a large number of investigations of TL properties of quartz has been performed, the TL-peaks at 100-110°C, 200-210°C and 350°C were especially well studied [8-11]. Emphasis on the experimental processes and annealing conditions were in focus and marked changes which show tendencies towards influencing the TL response and consequently the sensitivity of materials and quartz and glass properties have been noted [1,12]. Taylor and Lilley [13] for example, have pointed out that the reduction of TL intensity is due to thermal quenching such that its efficiency obviously becomes more at higher temperatures, and in the fact the luminesece efficiency is generally a temperature sensitive factor, efficiency decreasing with increase of temperature, due to the increased probability of non-radiative transitions due to killer centers [14,15]. The sample thickness was found to constitute another important factor that influences the temperature gradient and temperature lag especially at higher heating rates. Such an effect is in fact, a common problem for virtually all dosimetric analysis systems which inherent a setback of systematic error on the temperature scale due to differences in the temperature recorded by the thermocouple and the emitting sample surface that is lagging behind, by perhaps some 50°C [16,17]. This effect may consequently lead to an overestimate of the activation energy values by about 10% which can explain the variations in the observed experimental determinations [18]. The annealing processes, on the other hand, may also bring about sometime undesired results, i.e. enhancement or reduction of TL sensitivity of TL-peaks. The literature is full of examples and for quartz; the trigonal a-quartz is the stable modifications under normal conditions. At larger temperatures, e.g. 573 and 870°C, quartz converts into hexagonal beta and trimdymite modification, respectively [9]. Theoretical studies, on the other hand, were devoted for establishing TL-models and devising possible methods of evaluating related parameters [9,19]. Many have been dedicated to the TL of silica glass and the literature is available on the TL of pure and doped a-SiO_2 with impurities [20]. Nevertheless, some common features were found in most of the glow curves of quartz, silica and silica films [21-23].

To this end, TL characteristics related to trap structure and thermoluminescence kinetic

Table1. Summary of TL characteristic of quartz samples of various heating rates

Quartz variety	Apparent major TL-peaks	Reference
BDH Quartz: β=2.0°Cs^{-1},	T_M: 90, 215, 325°C	Carvalho et al. (2010) [4]
Natural Quartz, β=1.0°Cs^{-1},	T_M: 82, 148, 200, 303°C	
Nigerian, 2.0°Cs^{-1},	101, 170, 226, 324°C	Ogundare et al. (2006), [6]
Synthetic Quartz: β=1.0°Cs^{-1},	T_M: 96.0, 193, 296°C	Yazici and Topaksu (2003) [10]
Arkansas Quartz: β=2.0°Cs^{-1},	T_M: 106.2±5.5°C	
BDH Quartz: β=2.0°Cs^{-1},	T_M: 102.4±5.5°C	
Norwegian Quartz: β=2.0°Cs^{-1},	T_M: 104.8±2.6°C	de Lima et *al.* (2002), [37]
SOT Quartz: β=2.0°Cs^{-1},	T_M: 102.3±5.1°C	
Arkansas Quartz: β=4.0°Cs^{-1},	T_M: 370, 420-470°C	
	T_M: 97, 147, 197°C	Kitis et al. (2003), [40]
BDH Quartz: β=2.0°Cs^{-1},	T_M: 102.4±5.5°C	
Norwegian Quartz: β=2.0°Cs^{-1},	T_M: 104.8±2.6°C	Adamiec (2005) [41]
SOT Quartz: β=2.0°Cs^{-1},	T_M: 102.3±5.1°C	
Arkansas, Norwegian and Sea sand: β=2.0°Cs^{-1},	T_M: 170, 220, 320°C	Pagonis et al. (2002) [42]
Australian Quartz: β=5.0°Cs^{-1},	T_M: 100, 180, 220, 260, 302, 350, 450°C	Franklin et al. (1995) [43]
γ-irradiation		
Chert Quartz: β=3.37°Cs^{-1},	T_M: 98.6-105, 325, 375°C	Ankama et al. (2011), [44]
Quartz: β=2.0°Cs^{-1},	T_M: 89-120°C	
Arkansas Quartz: β=4.0°Cs^{-1}, 5.0-°C s^{-1}	T_M: 110, 230, 270, 325, 375°C	
	T_M: 110,225,265,325,385°C	Preusser et al. (2009) [45]

parameters, of natural crystalline (c-SiO_2) quartz and synthetic amorphous silica glass(a-SiO_2) prepared by sol-gel technique after irradiation using beta source, are measured in this work and compared with values from the literature and the kinetic parameters are reported.

2. MATERIALS AND EXPERIMENTAL METHODS

The samples used in this study were natural quartz (Brazilian natural quartz) and silica glass prepared by sol-gel technique. It is generally noted that the conventional method of preparing glass is to use the melting technique, see e.g. [24]. An alternative procedure of using high temperatures methods is to adopt the sol-gel procedure followed by, e.g. Mukasa et al. [25]. This procedure obviously has made possible the organic modification of silicon compounds, which cannot withstand high temperatures. Samples were synthesized from the starting solution, tetraethyloxysilane (TEOS), with molar ratio: (TEOS:C_2H_5OH:H_2O:HF) equals to: (1:4:4:0.05). The solution was mixed and stirred well for about 1 hour at ambient temperature, using a magnetic stirrer, until it became transparent. The solution was poured into in a cylindrical plastic container that was covered with an aluminum pinned holes foil. The container was dipped into a water bath that was held at 60°C for 24 h to favor the polymeric route over the colloidal one, and induces hydrolysis and condensation, the period at which the volume becomes about one third of its original volume. Details of the reactions involved during hydrolysis, indicate that alkoxy group (OR) are replaced with the hydroxyl group (OH) and the condensation reactions involve the sylanol groups to produce siloxane bonds Si-O-Si plus by products: Alcohol (ROH) or water. However, the ratio of hydrolysis to condensation and the associated polymerization reactions determine the properties of the gel and the material resulting from that gel. The gel was further dried at 200°C for about 2h and was then slowly cooled down and brought to room temperature (RT).

The resulting homogeneous mix prepared from sol-gel technique was in the form of coarse grained particles. The powder was grinded using a mortar and sieved using a mesh of particle size less than ≤ 75 μm. Samples used in the measurements were shaped out in the form of circular discs, each of mass 15 mg, and pressed under a 1.0 ton pressure with dimensions: 4.5 mm diameter and thickness about 1mm. All samples were then annealed at different

temperatures up to 1100°C in a platinum (Pt) crucible for 2 h using a microprocessor controlled furnace and then cooled slowly to RT prior to irradiation.

Irradiations were carried out at RT with a calibrated ^{90}Sr-^{90}Y-β-particles emission source, using VINTEN Model 623 automatic dosimeter irradiator of nominal activity 1mCi which, delivers dose to the samples at a rate of 2.87μGy s^{-1}.This test dose was found suitable for stability conditions and repeated measurements indicate that the annealing temperature results in the detected GL-peaks. The delivered test dose to the samples was varied up to 2Gy, in steps of 0.5Gy. This same test dose was also found to reveal all TL-peaks in the GL-curve of sample type (prepared by sol-gel technique. The read out stage was made using Harshaw Model 3500 TLD reader, with planchet heating system controlled by Windows®–based Radiation Evaluation and Management System (Win-REMS), a proprietary of Thermo Electron Corporation RM&P's [26]. The TL-signal representing the Glow (GL-) curves were recorded using a suitable software, Win-REMS, interfaced to a personal computer (PC), for further analysis. All GL-curves were read using a linear heating rate of 2°Cs^{-1}, from room temperature up to 380°C with preheat temperature (T_p) set at 80°C. This temperature was found ample to eliminate the more rapidly low temperature fading peaks in the GL-curves and make the higher temperature end of the signal visible. This, however, ensures consistency within our measurements, except for those varying heating rate experiments where, constant but varied heating rates between 2 and 10°Cs^{-1} were used. The temperature variation in the range from ambient to 673K (400°C) was 2K.

The use of more than one technique and/or an alternative approach may not only enhance the validity of the results and conclusions but also becomes indispensable when one fails due to sensitivity, availability and resolution limitations. The approach followed was to make use of complementary available techniquessuch as Energy Dispersive Spectroscopy (EDS) and Scanning Electron Microscopy (SEM) to facilitate comparison between measurements. More details about the preparation procedure, conditions of the sol-gel method, and measurement system and techniques are found elsewhere [27].

3. ANALYSIS OF THERMO-LUMINESCENCE GL-CURVES

Thermoluminescence analysis which governs the behavior of the GL-curves contains inherent overlapping peak features and therefore, requires de-convolution of the total glow (GL-) curve. Various peak components are extracted to reveal mechanisms dominating charge transfer and recombination processes. Data analysis, however, involves determining the trapping parameters based on available defect models and related techniques, see e.g., [28-31]. The common practice procedure of TL-analysis is to obtain the trapping parameters based on the general order kinetic rate equation, namely:

$$I(T) = s''n_o e^{-(E/kT)}\left[1 + \frac{s''(b-1)}{\beta}\int_{T_o}^{T} e^{-\left(\frac{E}{kT'}\right)}dT'\right]^{-\frac{b}{b-1}} \quad (1)$$

Where: n_o= initial concentration (cm^{-3}) of trapped charge carriers at time *t=0* and initial temperature $T_o = 0K$. *s* = a constant characteristic of the electron trap, called the pre-exponential frequency factor or attempt-to-escape frequency" (s^{-1}). This parameters proportional to the frequency of the collisions of the electron with the lattice phonons. Typically the maximum values of s correspond to the values of the lattice vibration frequency, i.e. 10^{12}–10^{14} s^{-1}, *s′* = the effective pre-exponential factor for general order kinetics ($cm^{3(b-1)}$ s^{-1}), $s'' = s'n_o^{(b-1)}$ = an empirical parameter acting as an "effective" frequency factor for general-order kinetics (in s^{-1}), β = heating rate (in $K.s^{-1}$); assumed linear: $T = T_o + \beta t$, *E* = activation energy or trap depth (in eV); *b* = kinetic order; *k* = Boltzmann constant (=$8.617x10^{-5}$ $eV.K^{-1}$); and *T* = final temperature (in K).

To this end, it is suffice to introduce here the methods of analysis adopted in TL-analyses of the GL-curves, based on the developed theoretical models. A brief description which is crucial to provide a basis for interpretation and evaluation of the results is given below.

3.1 Curve Fitting Method

The common practice procedure of total computerized GL-curve de-convolution (TGCD) to separate inherently overlapping features is an active area of interest and has become more important in view of its numerous applications, such as: Dating, dosimetry and defect studies. The method is based on solving equation (1)

numerically using a standard software, e.g. Peakfit or Origin. The procedure basically follows a semi empirical approach and depends on approximate positions of the most prominent peaks in the GL-curve and initial estimates of the parameters representing charge release and recombination mechanisms [32]. This approach ensures that the peak centroids, intensity and widths, are all not disturbed by the analysis. An iteration procedure was followed which minimizes the sum of the squares between the experimental GL-curve and the fitted one by calculating fitting coefficients of each de-convoluted peak. Examples of the total GL-curve de-convolution procedure are presented in terms of the separated peaks, their sum. Comparison between the computed theoretical curves and experimental ones, represented in terms of the residue curves are also shown on top some extracted curves, see e.g. Figs. 6 and 7. Deviations between the measured and fitted data indicated that reproducibility, in obtaining new values from initial curve fitting estimates are always maintained to better than 2%. The output of the calculation which represents the kinetic parameters, namely the trap depth (*E*), thermal or activation energy which is the energy needed to free the trapped electrons, the temperature at maximum (T_M), kinetic order (b), the frequency factor (s) and lifetime (τ) are listed in Table 2.

The frequency factor values were determined from the GL-curves measured at different heating rates by determining T_M for each TL-peak. Once the kinetic orders and activation energy values are determined, the frequency factor is calculated from the general order kinetic equation, given by [33], namely:

$$\frac{\beta E}{kT_M^2} = s\left[1 + (b-1)\frac{2kT_M}{E}\right]e^{-\frac{E}{kT_M}} \qquad (2)$$

Which reduces for first and second order, respectively to:

$$\frac{\beta E}{kT_M^2} = se^{-\frac{E}{kT_M}} \qquad (3)$$

$$\frac{\beta E}{kT_M^2} = s\left[1 + \frac{2kT_M}{E}\right]e^{-\frac{E}{kT_M}} \qquad (4)$$

Accordingly, the trap depth, E is found from the slope of the straight line obtained when the logarithmic term $ln({T_m}^2/\beta)$ is plotted against $1/kT_m$ [19]. The frequency factor values obtained from the intercept of the slope, are listed in Table 3.

4. RESULTS AND DISCUSSION

4.1 Structure of Pure Silica Glasses (SiO_2)

Typical X-ray diffraction (XRD) pattern recorded by means of stepwise method, within the angular range from 10º to 80º and counting time of 0.4s of both types of SiO2-glasses, as prepared and annealed at 1100°C/2 h in a Pt- crucible, are shown in Fig. 1. The presence of the crystalline phase (natural quartz) is clearly noted to match the sharp peaks observed at 20.77º, 26.62º, 50.26º, 60.02º and 68.27º. This indicates that natural quartz which exhibits well defined X-ray diffraction patterns is of crystalline structure. On the other hand, comparison between the XRD patterns obtained from SiO_2-glass samples prepared by sol-gel method without annealing and those after treatment at 1100°C/2 h, shows the presence of a broad peak with inherent group peaks structure illustrating the amorphous phase of the powder material obtained, with main peaks detected near 23.13º and 21.26º respectively. The tendency of the annealed pattern to shift towards lower angles accompanied by narrower peak feature gives good indication of movements towards crystalline structure or better orientation; is always consistent and in agreement with reported data in the literature [10,11,34]. Also, the beta rays irradiation caused partial

Table 2. Determined crystallite size of natural quartz and silica glass prepared by sol-gel both at RT and annealed at $1100^oC/2$ h

XRD-Analyses of silica-glass prepared by:	Position of angle ($2\theta_m$)		FWHM - β (=radians)		Crystallite Size [$D=0.9\times\lambda/\beta\times\cos(\theta_m)$]($A^o$)	
	RT	1100°C/2h	RT	1100°C/2h	RT	1100°C/2h
Sol-gel	23.13^o	21.26^o	11.21^o (=0.2)	7.99^o (=0.14)	7.082	10.085
Natural quartz	P_1	P_2	0.41^o (=0.007)	0.2^o (=0.003)	201.56	475.37

transformation from amorphous to crystalline. The crystallite sizes for the hosts were evaluated based on the Sherrer equation presented in Eq. (3), namely:

$$d = \frac{0.9\,\lambda}{\beta\cos\theta} \qquad (5)$$

The determined crystallite sizes are listed in Table 2. Clearly, one notices that the annealing temperature (T_a) affects the size in such a way that as T_a is increased the particle size tends to increase too.

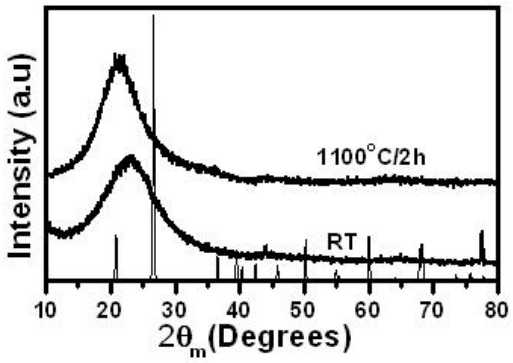

Fig. 1. XRD pattern of silica glass: Crystalline as obtained from natural quartz (sharp lines) and amorphous phase as obtained from glass prepared by sol-gel technique at RT and after annealing at$1100^{o}C/2h$

In Fig. 2, the Energy Dispersive Spectrum (EDS)and (SEM) image of as prepared amorphous SiO_2 powders with particle $\sim 50\,\mu m$ size distribution and annealed at$1100^{o}C/2\,h$, is shown.The EDS spectrum reveals the presence of the main components constituting quartz, namely silicon and oxygen. In fact, oxygen exists in amounts exceeding the stoichiometric ratio of $Si:O = 1:2$. This is attributed to the presence of water and $-SiOH$ groups during preparation conditions and its retention in the final product. The spectrum on the other hand which, did not show any presence of carbon traces or fluorine ions gives worthy indications that these ions have well been removed and washed away from the original solution during the preparation and drying phases.

4.2 Effect of Annealing Temperature

The effects of high temperature annealing between 900 and 1100°C and consequently influence on TL-characteristics were investigated for a constant annealing time of 2 h, in Fig. 3. The curves which are distinguished by features of crystalline behavior are characterized by the detection of two distinct groups of TL-peaks within the temperature range between room temperature and 380°C. This gives evidence that apart from the preparation conditions, the basic material and its components are effective in light production and result in the formation of two group TL-peaks with apparently inherent overlapping features. Generally, the data reveals the detection of two sharp TL-peaks (150°C and 200°C), for quartz, while two broad peak structures of varying intensities are detected near (150°C and 300°C) with SiO_2-sol-gel method, as shown in Fig. 4. The data presented indicate influence of TL-response on the annealing temperature, accompanied by a marginal shift of TL-peaks maximum intensity by some 8K, to lower temperatures as seen with the annealing at 1100°C. One reason for the shifts in TL-peaks maximum temperature can be due to cluster formation/annihilation processes accompanied by wider/narrower distributions after annealing. The intensity of the main observed peaks of quartz detected near 150 and 200°C was observed to increase with the annealing temperature. As the temperature is increased from 900 to 1100°C, the first (second) TL-peak detected at 150°C (200°C) was noted to increase by about 2.7 (1.6) times. The sol-gel annealing data at 1100°C indicate an increase of TL-intensity of the first peak near 150°C by almost three times while the second peak detected near (300°C) was noted to be marginally affected. These high temperature annealing data convey important information, where the TL-response is markedly influenced by the annealing temperature, as expected; the temperature at maximum is insignificantly affected. The data presented in Fig. 3, additionally, shows no influence of various thermal treatments on the GL-curves, or formation of new trapping states or new luminescent centers. The effect of TL after high thermal annealing, on the other hand, may depend on the cooling rate. However, thermal quenching which is due to slow ionic processes, on contrary to the much faster electronic processes involved in thermal quenching, is minimal [19,34-37]. Nevertheless, sensitivity changes are associated with alterations in the concentration of recombination centers and the presence of the second peak detected near 300°C is attributed to phase transformation in the synthesized quartz. The broad peaks are, however, typical of the amorphous phase of

materials, where the activation energies of the traps form continuous distributions rather than a spectrum of discrete values, in contrary to the case seen in crystalline materials [38].

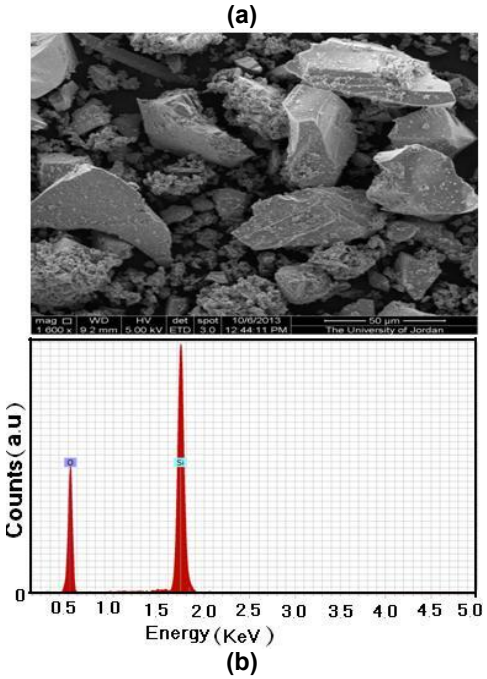

Fig. 2. (a) SEM image of amorphous SiO_2 annealed at 1100°C/h, and (b) Energy Dispersive Spectrum (EDS) of the SiO_2. The detected peaks represent the main constituents of quartz glass, namely Si and O

4.3 Dependence of Peak Positions on the Heating Rate

The effect of heating rate on the normalized glow curve intensities of TL-peaks is illustrated in Fig. 5. All samples were subjected to annealing at 1100°C for 2 h and the heating rate effect was studied for dose of 2Gy. The strong overlap with comparable intensities constituted a major point in our determination imposes limits on the number of TL-peaks to be used in the de-convolution process. It is worth mentioning that the approach followed is based on a minimization procedure that calculates the sum of the squares of fitting coefficients and the total simulated curve is then compared with the experimental data by evaluating the residues. The GL-curves were found to fit best using five and six TL-peaks labeled P_1 to $P_5$for natural quartz, while P_1 to P_6 for synthesized quartz is, as shown in Figs. 6 and 7 with the presence of two clear dosimetric TL-peaks group structures TL-peaks, detected near T_M=150°C and 200°C; as expected from this material for quartz. The results of the de-convolution procedure are also shown in Figs. 6 and 7, and both figures show TL glow peaks of crystalline and synthesized quartz samples are not symmetric, as shown in Fig. 8 with the determined trapping parameters listed in Table 3.

It is generally noticed that as the heating rate is further increased, shifts of TL-peaks maxima towards higher temperatures accompanied by a decrease of TL-intensity are observed, as shown in Fig. 9. The TL-response within the GL-curve was normalized to the lowest heating rate, i.e. $2°C.s^{-1}$. Additionally, the influence of the heating rate on TL-peak height intensities which inherent more than one TL-peak corresponding to more than one trap is approximately equal. This gives evidence that no effect on the trap population is taking place, and the effect of heating rate is only to alter the mechanism of trapping processes. By reference to the de-convolution procedure carried out, the TL characteristics related to trap parameters of different emission TL-peaks are thoroughly explored. Such states are mostly associated with electron-hole (i.e. exciton) pairs and oxygen defect sites related to shallow and deep trap centers [7]. The peaks are, however, described by the trapping, parameters, namely E, T_m, b, n_0 and calculations of frequency factor (s) from Eq. (2) and lifetime (τ), at ambient temperature of 18°C, with trapping parameters listed in Tables 3 and 4. The first peak (P_1) for both types of quartz materials detected near T_m=150°C, is known to be due to band-to-band transition of electrons from the minimum of the conduction band to valence band maximum (VBM). Peak two (P_2) with T_M=200°C, on the other hand, is attributed to relaxation of an exciton formed during ionization at a broken Si-O bond [7]. Emission of self-trapped exciton (STE) occurs as results of direct carrier recombinations or via an oxygen vacancy [28]. The other peaks, P_3, P_4 and P_5 are due to E´-centers, namely$E_1^{'}$,$E_2^{'}$ or $E_4^{'}$ centers, respectively [21]. The E´-center comprise an unpaired electron of a single silicon atom bonded to just three oxygen atoms in the glass network. Such a generic E´-center is often denoted by ≡Si●, where the three parallel lines represent three oxygen separate bonds to one silicon atom and the dot denotes the unpaired electron. This defect center is entitled simply by a neutral oxygen vacancy, often denoted by ODC and indicated generally as≡Si−Si≡. The presently accepted model for $E_1^{'}$ center is also an oxygen vacancy with an unpaired electron located on

one of two non-equivalent Si atoms at sites(I) and (II). Silicon at site (I) results from the lattice distortion around the vacancy. The $E_2^{'}$-center, is also an oxygen associated with a proton. The electron, in this case, is located on Si atom at site (II). The $E_4^{'}$center is an oxygen vacancy with a hydride ion bonded to a Si atom at the different site, i.e. (I). A trapped electron is, however, shared between Si at both sites, spending most of its time on Si at site (II). It is worth noting that these E´-centers can form sub-band states extending from shallow to deep levels in the band gap of SiO_2 indicating that they are considered to be thermally connected traps and electrons can flow between the centers. It worthwhile mentioning that various authors have assigned these defect states to be due to impurities such as OH^-, H^+, or to non-bridging oxygen induced by irradiation. In addition, the trapped electron shared between the two sites (I) and (II) implies that the trapped electron spends most of its time on the first site, i.e. site (I), with three bonds linked to the glass network structure.

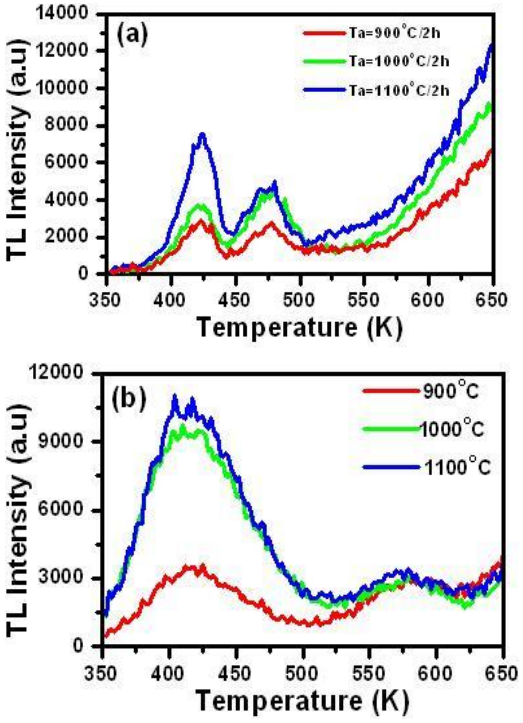

Fig. 3. Typical GL-curves of 0.5Gy β-dose irradiation both silica glasses: (a) natural and (b) prepared by sol-gel method, illustrating the effects of 2h annealing at different temperatures. Glow curves are measured at a constant heating rate of $2Ks^{-1}$

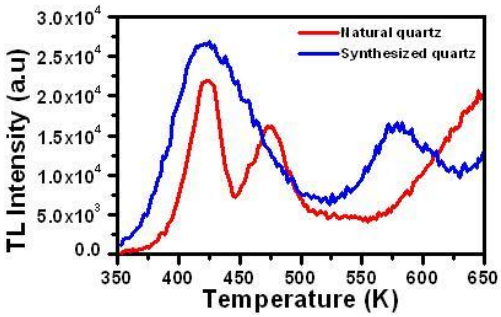

Fig. 4. Typical TL GL-curves showing the noted variations of TL-intensity between samples annealed 1100^oC for 2h and representing natural quartz and synthesized samples using sol-gel technique. Measurements are recorded at a constant heating rate of $2Ks^{-1}$ after imparting a total dose of 2Gy

The changes in peak temperatures T_m as a function of heating rate for annealing temperature at 1100^oC, are shown in Fig. 10. It is clearly seen that for each TL-peak, T_m increases with the heating rate; an expected result. The variable heating rate (VHR) method proposed by Chen and Winer [19] is one method to determine kinetic parameters of any distinct TL-peak. According to Eq. (2), the VHR method allows one to estimate the trap depth and frequency factor; determined from the plot of $ln(T_m^2/\beta)$ against $1/T_m$, as shown in Fig. 11 and their values are listed in Table 4.

From Tables 3 and 4, *E* and *s* values are determined by the (TGCD) and VHR methods. Comparison of *E* and *s* values obtained by the VHR method is, however, more complex; *s* values are always 3-4 orders of magnitude different for all methods [37]. In general, there exist large disparities between the results of different methods for high temperature glow peaks. These are probably due to artifacts in the method related to the large number of inherently overlapping peaks, which limits the accuracy of the determination of kinetic parameters [10].

4.4 Effect of Irradiation Dose

The behavior of TL-intensity of both natural quartz and synthesized a-SiO2 glass silica quartz is shown as function of β-irradiation dose in Fig. 12. The data articulates the logic and provides informations that illustrate the maximum temperature is insignificantly influenced by the

dose indicating that TL-kinetics are represented by nearly first order mechanisms. The data also gives indication that within the range of the doses investigated, both quartz and a-SiO_2 silica glass exhibit a linear response as a function of dose with quartz showing a lower sensitivity than silica quartz glass prepared by sol-gel technique as shown in Fig. 13. It is worth noticing that the order of kinetics results of the 150°C TL-peak of natural quartz displays an average value of b=1.10. On the other hand, the a-SiO_2 glass which contains inherent overlapping three TL-peaks centered near (138°C, 166°C and 195°C), respectively, display average kinetic order values of (1.24, 1.36 and 1.56). These values are, however, inconsistent with the values obtained from quartz, and follow general order kinetics, *with average value equals to 1.39eV*. The values of E, are respectively (=1.25±0.03eV) for quartz, and E (=0.80, 0.86 and 1.04±0.03eV) for a-SiO_2 silica glass. Although these values, free well with earlier literature values and may be used in the complex model [39]; the values of s appear to be different and display variations

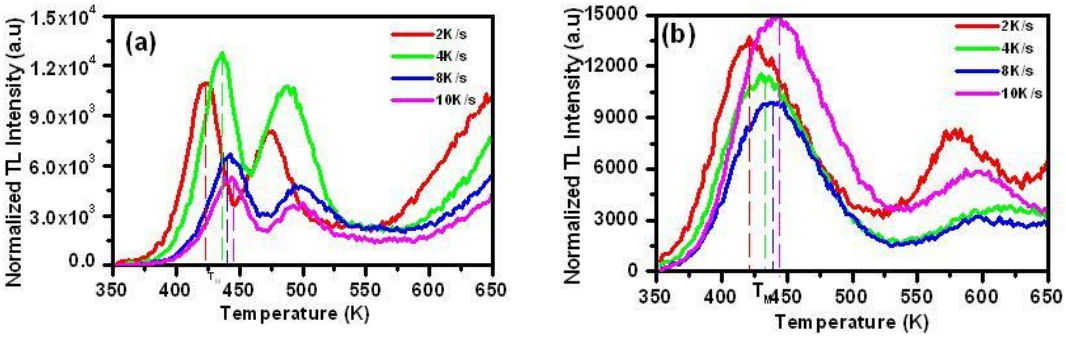

Fig. 5. Normalized glow curves at 1100°C for 2h of (a) natural quartz and silica glass (b) prepared by sol-gel method. GL-curves are measured at various heating rates after βirradiation up to 2Gy

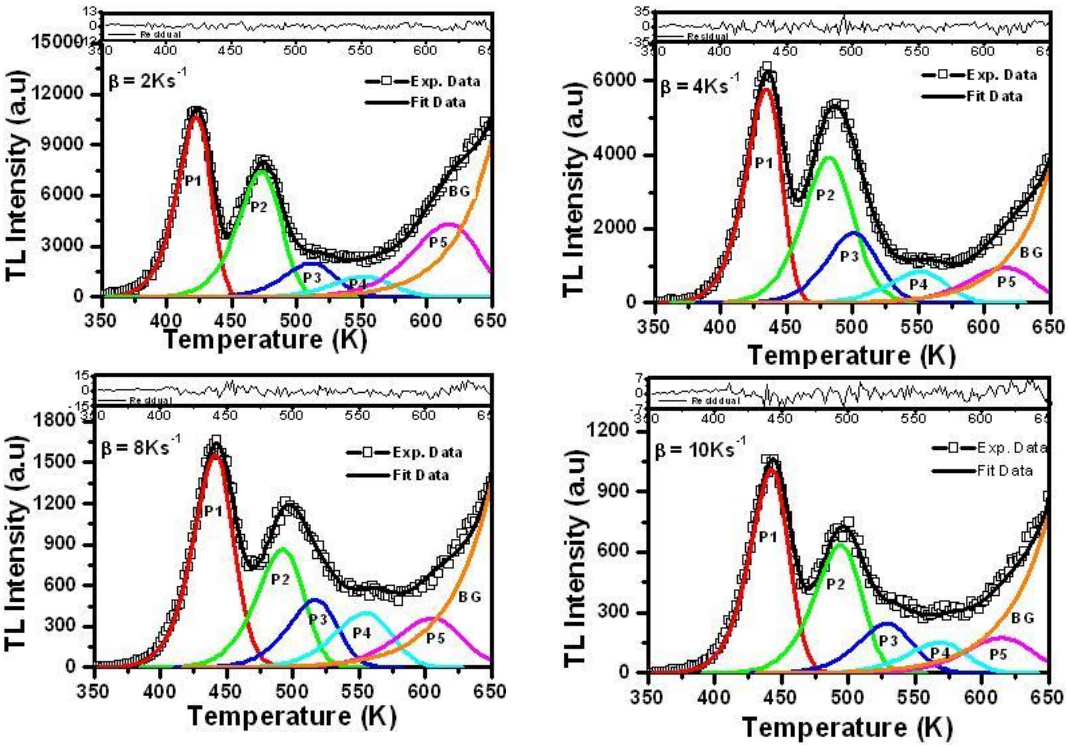

Fig. 6. De-convolution of normalized GL-curves of natural quartz obtained at different heating rates heating rates (HR) and following β-irradiation to a dose level of 2Gy

between 10^{10} to 10^{14} s^{-1}. In the more generalized models where the presence of competing traps in quartz are considered to account for enhanced sensitivity at higher doses, first order kinetics determined for the case of the 150°C peak, cannot be true for all situations. Incidentally, high concentrations of thermally disconnected traps lead to apparent first order GL-curves irrespective of the presence of re-trapping. Nevertheless, the simple test conducted in Fig. 11, emphasize non-first order kinetics through the dependence of TL-peaks positions on the irradiation dose. One notices that TL-peaks within the GL-curves are expected to change only with heating rate for b=1. Hence, for a constant heating rate, T_M should not be affected by other experimental parameters and should thus be fairly constant within the limits of experimental uncertainties. However, for b different from unity, and below the trap saturation points (the concentration of trapped electrons, n_o, is less than the concentration of traps, N_i), the peak temperatures are shifted to the lower temperature side with increasing dose levels. The data of Fig. 10 clearly show that TL-peak positions are insignificantly effected by the dose, for all doses, indicating that the GL-peaks in the glow curve nearly behave as first order kinetics. Indeed, our observation indicates that the kinetic order values are non-first order but; in fact are of general order.

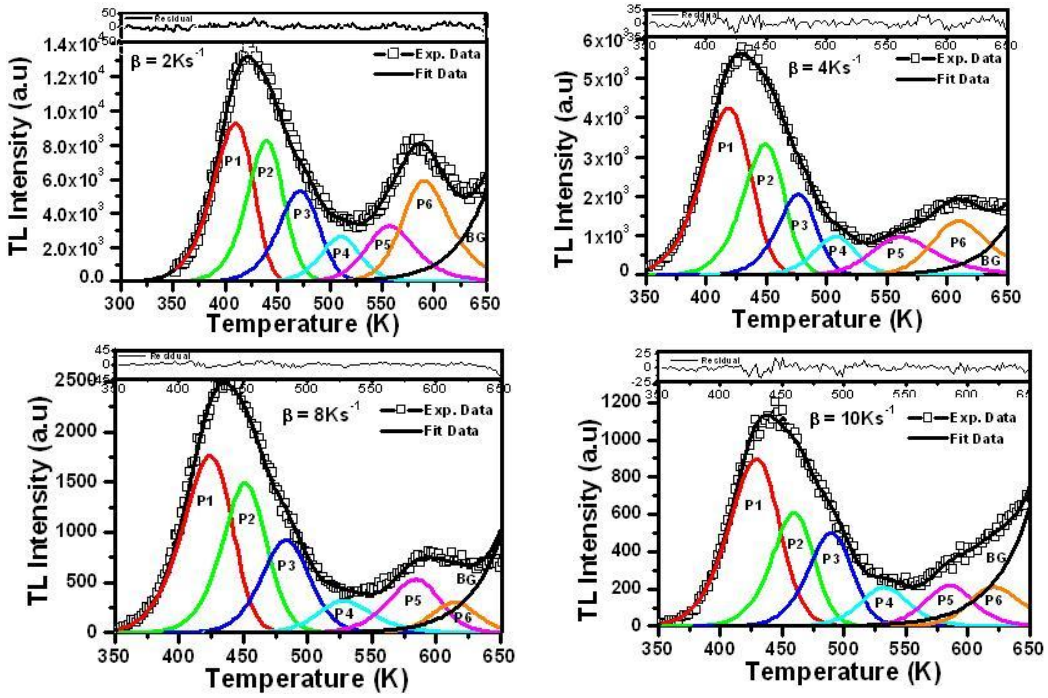

Fig. 7. De-convolution of normalized GL-curves of a-SiO_2: sol-gel obtained at different heating rate (HR) and following β-irradiation to a dose level of 2Gy

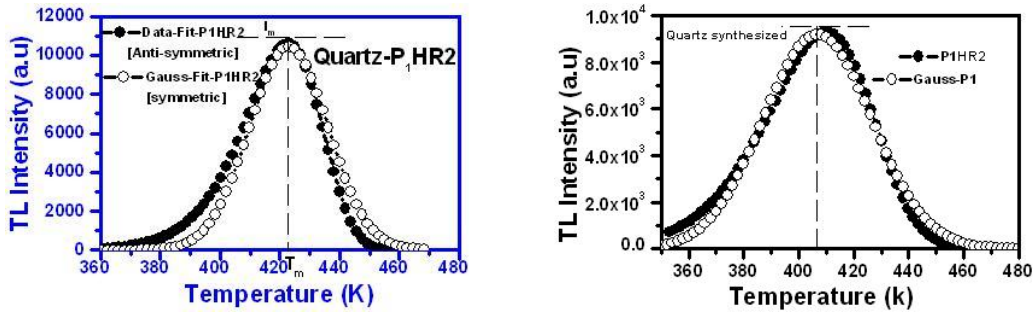

Fig. 8. Comparison of one of the TL glow peaks for both samples of the heating rate 2 Ks^{-1}, as a Gaussian function (open circle) and fitting of data of P_1 (solid circle)

Table 3. Trapping parameters of main TL-peaks of natural quartz and silica glass prepared by sol-gel method as determined total GL-curve de-convolution technique

β(Ks^{-1})	TL-Peak	Quartz					Sol-gel				
		E(eV)	T_m(K)	b	s(s^{-1})	*τ	E(eV)	T_m(K)	b	s(s^{-1})	*τ
2	P_1	1.24	423	1.10	9.57×10^{13}	12 m	0.76	410	1.10	2.31×10^{8}	17.49h
	P_2	1.28	473	1.22	5.7×10^{12}	82 y	1.10	439	1.38	5.49×10^{11}	7.91m
	P_3	1.29	505	1.34	8.75×10^{11}	808	1.12	472	1.56	8.75×10^{11}	1.00y
	P_4	1.30	539	1.35	1.54×10^{11}	7.73×10^{3} y	1.56	511	1.72	3.24×10^{14}	y1.04×10^{5}
	P_5	1.31	613	1.46	4.53×10^{9}	3.47×10^{5} y	1.70	557	1.40	3.00×10^{14}	y2.98×10^{7}
	P_6	--	--	--	--	--	2.10	590	2.50	1.13×10^{17}	y6.67×10^{11}
4	P_1	1.25	435	1.04	8.03×10^{13}	17.56 m	0.80	419	1.20	8.72×10^{8}	22.85h
	P_2	1.29	483	1.35	5.57×10^{12}	78.7y	1.14	449	1.27	1.61×10^{12}	1.11y
	P_3	1.30	512	1.08	1.43×10^{12}	734.48 y	1.38	477	1.31	1.05×10^{14}	243y
	P_4	1.32	551	1.25	2.26×10^{11}	9.17×10^{3} y	1.61	508	1.54	2.65×10^{15}	9.32×10^{4}y
	P_5	1.33	614	1.19	1.26×10^{10}	2.56×10^{5} y	1.64	561	2.5	1.21×10^{14}	6.60×10^{6}y
	P_6	--	--	--	--	--	2.15	609	2.48	1.63×10^{17}	3.41×10^{12}y
8	P_1	1.26	441	1.34	1.42×10^{14}	17.38m	0.87	424	1.22	9.68×10^{9}	1.40d
	P_2	1.29	492	1.22	7.67×10^{12}	88.52y	1.21	452	1.45	1.66×10^{13}	1.75y
	P_3	1.34	518	1.22	5.47×10^{12}	1.11×10^{3} y	1.40	483	1.65	2.18×10^{14}	260.97 y
	P_4	1.35	557	1.22	5.83×10^{11}	1.09×10^{4} y	1.65	528	2.14	3.07×10^{15}	3.96×10^{5}y
	P_5	1.35	605	1.22	6.33×10^{10}	1.43×10^{5} y	1.77	585	1.48	8.30×10^{14}	1.75×10^{8}y
	P_6	--	--	--	--	--	2.39	615	1.71	2.19×10^{19}	3.63×10^{14} y
10	P_1	1.26	442	1.22	1.71×10^{14}	15.64m	0.88	429	1.34	1.18×10^{10}	1.72d
	P_2	1.31	494	1.22	1.46×10^{13}	112y	1.22	460	1.34	1.52×10^{13}	2.85y
	P_3	1.36	529	1.34	4.39×10^{12}	2.15×10^{3} y	1.42	490	1.46	2.69×10^{14}	468.44 y
	P_4	1.37	568	1.22	6.46×10^{11}	3.36×10^{4} y	1.67	533	1.83	4.04×10^{15}	6.69×10^{5}y
	P_5	1.38	615	1.22	7.96×10^{10}	2.85×10^{5} y	2.03	585	1. 83	2.04×10^{17}	2.27×10^{10}y
	P_6	--	--	--	--	--	2.46	621	2.5	6.41×10^{19}	2.03×10^{15}y

With std. errors in: E= ±0.08%, T_m= ±5% and b= ±0.07%. Lifetime measurements are determined at ambient temperature (18^oC), and scale is in years unless specified otherwise, with (h=hours, d=days, m=months and y=years)

Table 4. Peaks maximum temperatures, T_m (K), and intensity, I_m (a.u), of the main dosimetric peaks of silica glasses prepared by sol-gel method. Associated heating rates, β (in Ks^{-1}) and determined activation energies E(in eV), frequency factors, s (in s^{-1}) and lifetime τquoted at ambient temperature of 18^oC (in years) are also included

β(Ks^{-1})	Quartz				Sol-gel	
	P_1		P_2		P_1	
	$T_m/(^oC)$	$I_m(a.u)$	$T_m(^oC)$	$I_m(a.u)$	$T_m(^oC)$	$I_m(a.u)$
2	150	10958	202	8074	150	8074
4	163	6343	216	5360	159	5360
8	170	6343	224	1144	166	1144
10	171	1032	225	686	170	686
E (eV)	1.23		1.28		1.24	
s (s^{-1})	2.357×10^8		3.178×10^8		2.835×10^{10}	
τ (y)	2.53×10^5		1.493×10^6		2.894×10^3	

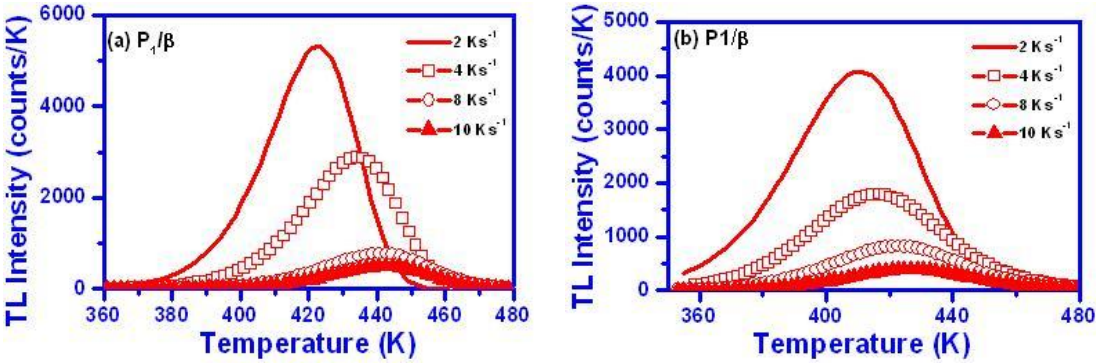

Fig. 9. TL glow peak of both samples for four different values β = 2, 4, 8, 10 K/s of the heating rate, and as a function of normalized by dividing by with their corresponding heating rates β, showing: variation with the concentration charge carriers after irradiation, while the peak maximum position of the TL glow curve shifts toward a higher temperature. The FWHM of the glow curves increases slightly with the heating rate

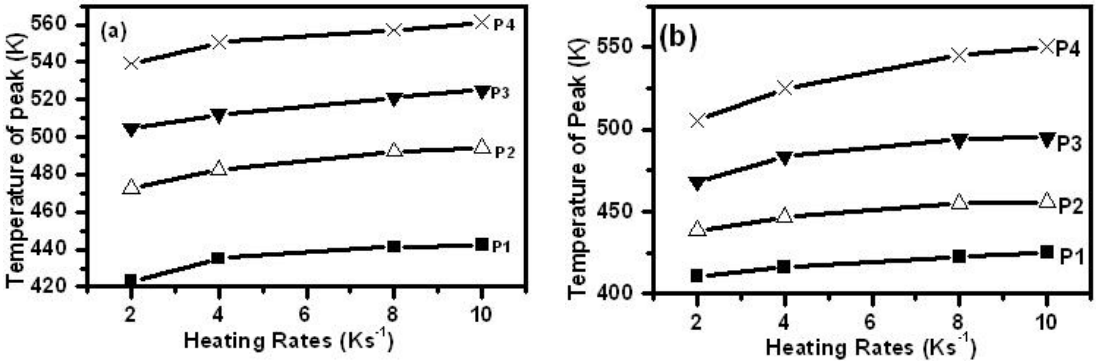

Fig. 10. Peak positions as a function of heating rate. Data are for: (a) natural quartz and (b) silica glass prepared by sol-gel technique

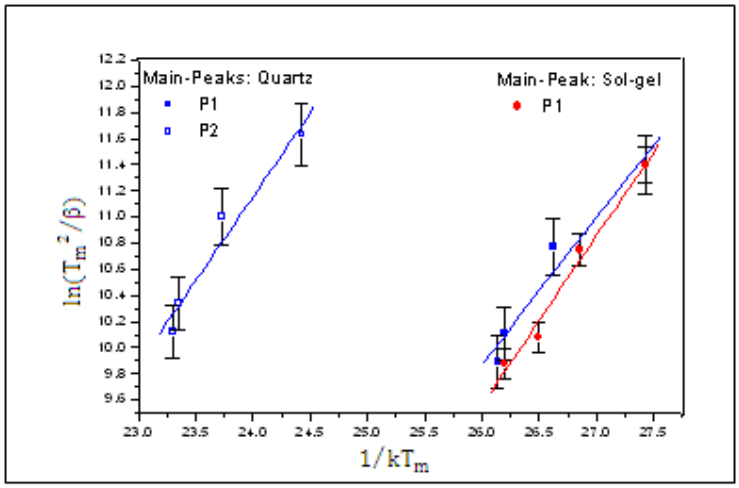

Fig. 11. Plot of $\ln(T_m^2/\beta)$ vs. $1/kT_m$ of both types of silica glass to obtain the activation energy; data are for quartz P_1 (□) and P_2 (■) and for sol-gel, P1 (■)

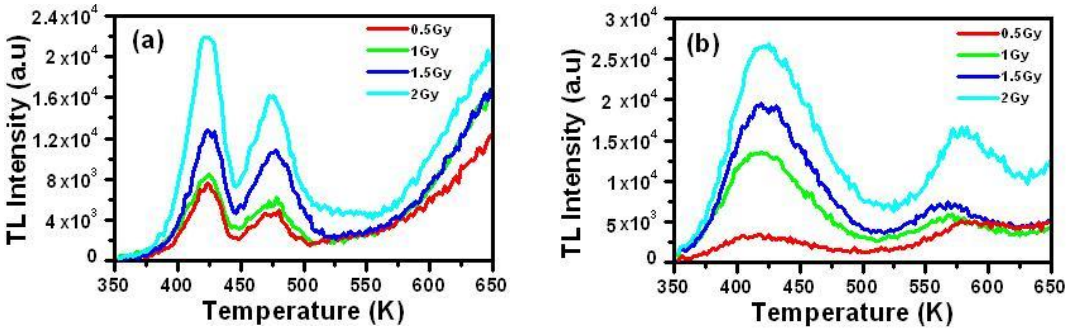

Fig. 12. Typical GL-curves at 1100^oC for 2h of (a) natural quartz and silica glass (b) prepared by sol-gel method. GL-curves are measured at a constant heating rate $2Ks^{-1}$ after βirradiation up to 2Gy

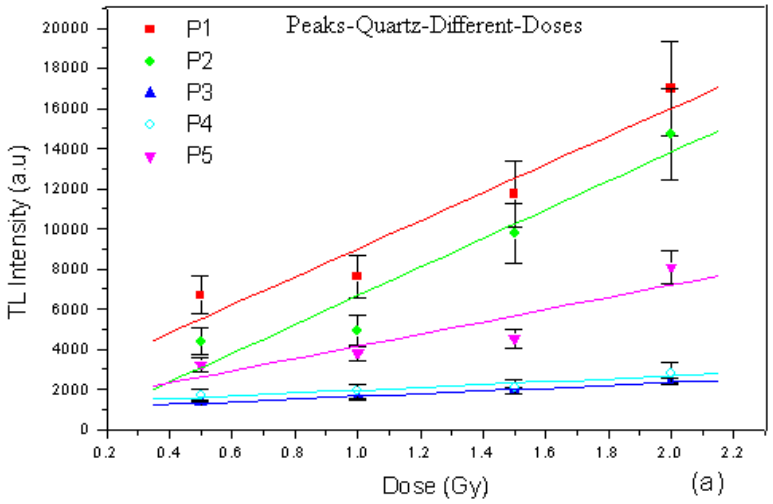

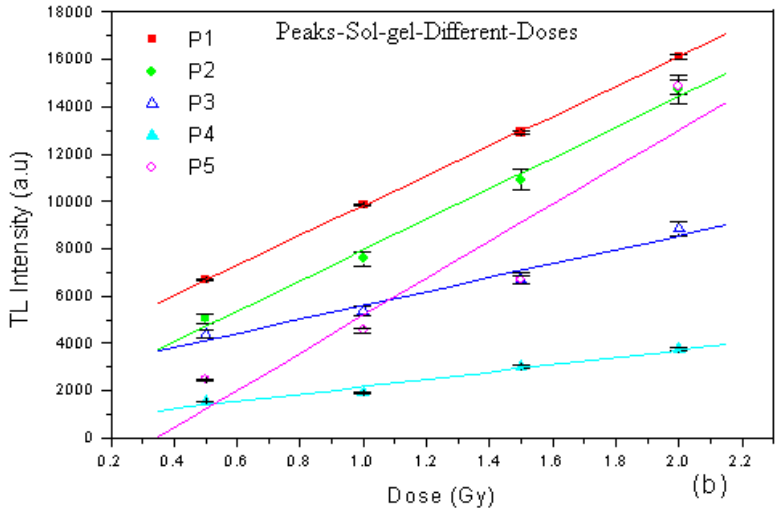

Fig. 13. Variation of TL-peaks annealed at $1100^{o}C$ for 2h,against different beta exposures of silica glasses: Natural glass in (a), and glass prepared by sol-gel method in (b). GL-curves measured at a constant heating rate $2Ks^{-1}$

5. CONCLUSIONS

Thermoluminescence properties of natural quartz and silica glass prepared by sol-gel technique occurring within an intermediate temperature range (RT - 50°C) were studied. Two main peaks were detected near 150°C (=423K) and 200°C (=473K) of natural quartz and near 150°C (=423K) and 300°C (=573K) with sol-gel technique, using a heating rate of 2°C/s. The region between two peaks, is more complex and was noted when observing the GL-curve of synthesized SiO_2, while after the two peaks natural SiO_2 samples. The response from the two main peaks within this temperature region indicates a linear increase with dose up to about 2Gy. The enhancement of TL-response was noticed to occur as a consequence of successive cycles of irradiations and heating treatments. Estimation of the lifetime of the detected peaks is crucial because as is long enough for estimating of age. Lifetime peaks of natural quartz are much longer than of silica glass prepared by sol-gel technique. Comparison with literature data indicates good match and agreement with reported trapping parameters. Improvement of TL-response and efficiency enhancement of light production of SiO_2-glass prepared by sol-gel technique will be the subject of another publication.

COMPETING INTERESTS

Authors have declared that no competing interests exist.

REFERENCES

1. Kiyk NG, Bulus E. Effect of annealing on determining of quartz by various heating rates method. Radiat. Meas. 2001;33:879-882.
2. Kitis G, Pagonis V, Carty H, Tatsis E. Detailed kinetic study of the thermoluminescence glow curve of synthetic quartz. Radiat. Prot. Dosi. 2002;100(1-4):225-228.
3. Nanjundaswamy R, Lepper K, Mckeever SWS. Thermal quenching of thermoluminescence in natural quartz. Radiat. Prot. Dosi. 2002;100(1-4):305-308.
4. Carvalho AB, Guzzo Jr. PI, Sullasi HL, Khoury HJ. Effect of particle size in the TL response of natural quartz sensitized with high gamma dose. Journal of Physics: Conf. Series. 2010;249.
5. Huseyin T, Necmeddin A. Effect of annealing on thermoluminescence peak positions and trap depths of synthetic and natural quartz by means of the various heating rate method. Chin. Phys. Lett. 2012;29(8).
6. Ogundare FO, Chithambo ML, Oniya EO. Anomalous behavior of thermoluminescence from quartz: A case of glow peaks from Nigerian quartz. Radiation Measurements. 2006;41:549-553.
7. McKeever SWS. Thermoluminescence in quartz and silica. Radiat. Prot. Dosi. 1984;8(1/2):81-98.

8. Petrov SA, Bailiff IK. The '110°C' TL peak in synthetic quartz. Radiation Measurements. 1995;24:519.
9. Hornyak WF, Chen R, Franklin A. Thermoluminescence characteristics of the 375°C electron trap in quartz. Phys. Rev. B. 1992;46:8036.
10. Yazici AN, Topaksu M. The analysis of thermoluminescence glow peaks of unannealed synthetic quartz. Phys. D: Applied Physics. 2003;36:620-627.
11. Topaksu M, Yüksel M, Dogan T, Nurd N, Akkaya R, Yegingil Z, Topak Y. Investigation of the characteristics of thermoluminescence glow curves of natural hydrothermal quartz from Hakkari area in Turkey. Physica B. 2013;424:27–31.
12. Polymeris G, Kitis G, Pagonis V. The effect of annealing and irradiation on the sensitivity properties of the 110°C thermoluminescence peak of quartz. Radiat. Meas. 2006;41:554-564.
13. Taylor GC, Lilley E. Rapid readout rate studies of thermoluminescence in LiF (TLD-100) crystals. J. Phys. D: Appli. Physics. 1982;15:2053-2065.
14. Nambi KSV. "Thermoluminescene its understanding and applications" Instituto De EnergiaAtomia, Saopaulo-Brazil; 1977.
15. Furreta C, Weng PS. Handbook of Thermoluminescence. World Scientific Co. Pte; 2003.
16. Betts DS, Couturier L, Khayrat AH, Luff BJ, Townsend PD. Temperature distribution in thermoluminescence experiments I: experimental results. J. Phys. D: Appl. Phys. 1993;26:843–848.
17. Betts DS, Townsend PD. Temperature distribution in thermoluminescence experiments. II: Some calculational models. J. Phys. D: Appl. Phys. 1993;26: 849–857.
18. Townsend PD, Rowlands AP, Corradi G. Thermoluminescence during a phase transition. Radiat. Prot. Dosim. 1997;27: 31–6.
19. Chen R, Winer SAA. Effect of various heating rates on glow curves. J. Appl. Phys. 1970;41(13):5227-5232.
20. Pandey A, Sahare P, Shahnawaz D, Kanjilal D. Thermoluminescence and photoluminescence characteristics of sol-gel prepared pure and europium doped silica glasses. J. Phys. D: Appl. Phys. 2004;37:482-846.
21. Martini M, Spinolo G, Vedda A. Thermally stimulated luminescence of thermally grown SiO2 films. Radiat. Eff. 1987;105: 107.
22. Martini M, Spinolo G, Vedda A, Arena C. Phosphorescence and thermo-luminescence of amorphous SiO2. Solid State Commun. 1994;91(9):751.
23. Bettinali C, Ferraresso G. Thermo-luminescence in vitreous sodium silicate. J. Chem. Phys. 1966;44:6.
24. Mehner HM Menzel, Nofz N. Hyperfine interactions. 2004;156/157:342-352.
25. Mukasa K, Ono H, Wakabayashi R, Ishii K, Ohki Y, Nihikawa H. Luminescence properties of sol-gel synthesized silica glass induced by an ArFexcimer laser. Phys. D: Appli. Physics. 1997;30:283.
26. Thermo Electron Corporation, Radiation Measurement & Protection, 26400 Broadway Ave. Oakwood Village, Ohio 44146 USA Thermo Suite, Thermo Electron Corporation RM&P ISO 9001 Quality System Certified, Model 3500 Manual TLD Reader with WinREMSTM, Operator's Manual.
Available:http://www.thermo.com\rmp
27. Khamis F. Synthesis and characterization of thermoluminescence properties of as prepared and doped SiO2- glass. Ph.D. Thesis, The University of Jordan, Physics Department, Amman, Jordan; 2014.
(Unpublished)
28. McKeever SWS. Thermoluminescence of solids. Cambridge University Press: Cambridge; 1985.
29. Halperin A, Braner AA. The trapping parameters are the activation energy (E), the kinetic order (b) and frequency factor, (f), Evaluation of thermal activation energies from glow curves. Phys. Rev. 1960;117:408.
30. Chen R, Kirsh Y. Analysis of thermally stimulated processes. Pergamon Press: Oxford; 1981.
31. Chen R, McKeever SWS. Theory of thermoluminescence and related phenomena. World Scientific: Singapore; 1997.
32. Horowitz YS, Yossian D. Computerized glow curve deconvolution: Application to thermoluminescencedosimetry. Radiat. Prot. Dosim. 1995;60:1–114.
33. Balarin M. Half width and asymmetry of glow peaks and their consistent analytical

representation. J. of Thermal Analysis. 1979;17:319.
34. Downs RT, Bartelmehs KL, Gibbs GV, Boysen MB Jr. Interactive software for calculating and displaying X-ray or neutron powder diffractometer patterns of crystalline materials. American Mineralogist. 1993;78:1104-1107.
35. Toktamis H, Yazici N. Effects of annealing on thermoluminescence peak positions and trap depths of synthetic and natural quartz by means of various heating rate method. Chi. Phys. Lett. 2012;29(8): 087802.
36. Pagonis V, Kitis G, Chen R. Applicability of the Zimmerman predose model in the thermoluminescence of predose and annealed synthetic quartz samples. Radiat. Meas. 2003;37:267-274.
37. de Lima JF, Navarro MS, Valerio MEG. Effects of thermal treatment on the TL emission of natural quartz. Radiat. Meas. 2002;35:155-159.
38. Kirish Y. Kinetic analysis of thermo-luminescence. Phys. Stauts Solidi (a). 1992;129(1):15.
39. Kantorovich LN, Fogel GM, Gotlib VI. A theoretical description of complex thermoluminescence curves. I. J. Phys. D: Appl. Phys. 1988;21(6):1008.
40. Kitis G, Pagonis V, Drupieski C. Cooling rate effects on the thermoluminescence glow curves of Arkanasas quartz. Phys. Status Solidi (a). 2003;198:312-321.
41. Adamiec G. Properties of the 360 and 550nm TL emissions of the '110oCpeak' in fired quartz. Radiat. Meas. 2005;39:105-110.
42. Pagonis V, Tatsis E, Kitis G, Drupieski C. Search for common characteristics in the glow curves of quartz of various origins. Radiat. Prot. Dosim. 2002;100:373-376.
43. Franklin AD, Prescott JR, Scholefield RB. The mechanism of thermoluminescence in an Australian sedimentary quartz. J. Lumin. 1995;63:317-326.
44. Ankama Rao K, Parvin Niyaz Sk, Poornachandra Rao NV, Murthy KVR. Thermally stimulated luminescence studies of silicate minerals. Scholars Research Library. Archives of Physics Research. 2011;2(4):89-93.
45. Preusser F, Makaiko LC, Götte T, Martini M, Ramseyer K, Sendezerad EJ, George J, Susino GJ, Ann G, Wintle AG. Earth-Science Reviews. 2009;97:196-226.

Peer-review history:
The peer review history for this paper can be accessed here:
http://sciencedomain.org/review-history/20578